PECULIARITIES OF C_{70} FULLERENE IN A BINARY MIXTURE OF XYLENE AND TETRAHYDROFURAN

U.K. MAKHMANOV[1,2], A.M. KOKHKHAROV[1], S.A. BAKHRAMOV[1], A.X. SHUKUROV[1], S.A. ESANOV[1], Z. BEKMURODOV[1], K.N. MUSURMONOV[1]

[1] Institute of Ion-Plasma and Laser Technologies, Uzbekistan Academy Sciences, 33, Durmon Yuli St., 100125 Tashkent, Uzbekistan
E-mail: urolmakh@gmail.com
[2] National University of Uzbekistan named after Mirzo Ulugbek, 4, Universitet str., 100174 Tashkent, Uzbekistan

Received May 1, 2025

Abstract. The optical and morphological properties of C_{70} fullerene in binary xylene/tetrahydrofuran solutions were systematically studied using UV-Vis absorption and Raman spectroscopy, refractometry, pycnometry, and dynamic light scattering (DLS). It was found that during storage of a molecular solution, the increase in intermolecular interactions and the onset of the self-assembly process of C_{70} molecules significantly affect the properties of the solution. A correlation was established between the formation of C_{70} nanoaggregates in solution and the changes in their properties (optical absorption, refractive index, density, and Raman spectra).

Key words: C_{70} fullerene, binary solution, C_{70}/xylene/tetrahydrofuran, absorption spectroscopy, refractive index, DLS, self-assembly.

DOI: https://doi.org/10.59277/RomJPhys.2025.70.617

1. INTRODUCTION

Fullerenes are unique materials in the rapidly developing fields of nanotechnology and materials science, exhibiting a wide range of applications [1–4]. The utilization of self-organization phenomena in fullerenes and their derivatives in solution to engineer tunable nanoscale and mesoscale morphologies in thin films continues to be a compelling focus for modern applications in field-effect transistors, photovoltaics, and biomedicine. A major advantage lies in the precise control over nanocluster formation processes, enabled by the distinctive properties of fullerenes and their derivatives [5]. These molecules exhibit exceptional stability, remarkable electrochemical activity, and a pronounced ability to self-organize, positioning them as promising candidates for the development of next-generation materials [6–8].

Binary solvents play a crucial role in synthesizing nanoaggregates of various sizes [9–10]. The incorporation of fullerenes into these solvents opens new avenues, significantly influencing the physicochemical properties of the solutions. The interaction between fullerenes and binary solvents represents a promising field for both fundamental research and practical applications. This study focuses on the properties of fullerenes that determine their effectiveness in binary solvents. Their ability to modify physical properties and reaction kinetics makes them candidates for optimizing industrial

processes [11]. Exploring the molecular interactions of fullerenes in binary solvents paves the way for innovation and technological progress.

In recent years, the self-assembly of C_{60} and C_{70} fullerenes in solution has been the subject of intensive research [10, 12–13]. The aggregation behavior of C_{60} and C_{70} has been studied in various solvents and their solutions, revealing the significant role of solvent polarity in the aggregation process [14]. Aggregation occurs through intermolecular interactions, with an equilibrium established between monomers and aggregates in solution. Relatively few studies have investigated fullerene aggregation in pure organic solvents [15–16].

This work presents the results of a study on the aggregation of C_{70} in a binary solution of xylene and tetrahydrofuran at various storage times and fixed fullerene concentrations. The unique time-dependent optical properties of C_{70} aggregates in solution are discussed.

2. MATERIALS AND METHODS

Crystalline C_{70} fullerene powder (≥99.8% purity) was obtained from SES Research (USA). The organic solvents used, xylene (C_8H_{10}) and tetrahydrofuran (C_4H_8O), both with ≥99% purity, were purchased from Sigma-Aldrich (USA). Both the C_{70} powder and solvents were used as received.

C_{70} solutions of known concentration were prepared by precisely adding measured amounts of aromatic and aliphatic solvents (xylene and tetrahydrofuran) to a pre-weighed sample of crystalline C_{70}. The solution was placed in a sealed glass vial and dissolved at room temperature using a magnetic stirrer (MS-11 H, WIGO, Poland) at a controlled speed of 3 Hz for 7 hours with simultaneous mechanical stirring.

The C_{70} powder was weighed using an analytical balance (EP214C, Ohaus Explorer Pro, Switzerland) with a resolution of 0.0001 g. All experiments were conducted at room temperature ($T \approx 24 \pm 1$°C).

The measurement of the precise refractive index (n) of the C_{70}/xylene/tetrahydrofuran system was performed at the sodium D_1 line wavelength of ~589.3 nm using a high-sensitivity digital refractometer PAL-BX/RI (ATAGO, Japan).

A portable densitometer Densito Pro (Mettler Toledo, Japan) was used to measure the density of the solution. The device has a measurement range of up to 3.000 g/cm³, accuracy of ±0.001 g/cm³, repeatability of 0.0005 g/cm³, resolution of ±0.0001 g/cm³.

UV-Vis absorption spectra of the C_{70} solutions were obtained using a double-beam spectrophotometer (UV-2700, Shimadzu, Japan) with a spectral resolution of 0.1 nm. Measurements were taken over a wavelength range of approximately 185 to 900 nm.

The distribution characteristics of the dispersed phase of fullerene C_{70}, including the average hydrodynamic size and particle concentration in solutions, were analyzed using dynamic light scattering (DLS) with a Zetasizer Nano ZEN3600 system (Malvern Instruments Ltd., UK).

The Raman spectra of fullerene solutions were recorded using an InVia Raman spectrometer (Renishaw, UK). A Cobolt CW 532 nm DPSS laser served as the excitation source, operating at a wavelength of 532 nm.

3. DISCUSSION

Changes in the density of fullerene solutions during storage can be attributed to several factors, including chemical reactions and aggregation. Over time, fullerene molecules may undergo interactions with solvent components or other impurities present in the solution. The latter can alter the molecular structure of the fullerenes, leading to the formation of new compounds (nanoclusters) with densities different from the initial fullerene solution.

As shown in Table 1, the density of the solution gradually decreases with increasing storage time. This indicates that fullerene molecules tend to aggregate or form clusters in solution, particularly at higher concentrations or under specific conditions. Such aggregation behavior can affect the effective density of the solution, as aggregated molecules may occupy a smaller volume compared to individually dispersed molecules.

Table 1

Change in the refractive index and density of C_{70}/Xy/TGF solution over time. The volume fraction of solvents is 0.95:0.05, respectively, C_{70} concentration is ~ 0.2 mg/ml

Time	Refractive index (*n*)	Density, g/cm³
1st day	1.4218	0.8840
5th day	1.4186	0.8805
10th day	1.4183	0.8750

The next stage was devoted to the study of the refractive properties of solutions, which served as the most important parameter for assessing the change in refractive index and understanding the intermolecular interactions of the components. The refractive index (RI) of fullerene solutions reflects intermolecular interactions between the solute and solvent. Fullerene aggregation, particularly at high concentrations or under specific conditions, influences the RI. Table 1 presents experimental RI values for C_{70} solutions in a xylene/tetrahydrofuran solution at various storage times. A decrease in RI is observed during subsequent storage of the solution for up to 10 days. This is attributed to increased intermolecular interactions and the onset of C_{70} self-assembly. The formation of C_{70}– C_{70} and C_{70}–solvent bonds enhance intermolecular interactions, leading to the formation of nanoclusters. The appearance of large clusters leads to an increase in the transparency of the solution and a decrease in the refractive index of light.

3.1. ABSORPTION SPECTRA

Solvent effects on the absorption spectra of organic compounds manifest as changes in the position, intensity, and shape of absorption bands, resulting from altered intermolecular interactions and the energy difference between ground and excited states.

Figure 1 shows the evolution of the UV-visible absorption spectra of C_{70} in a xylene/tetrahydrofuran solution over different storage periods. The absorption spectra are highly dependent on storage conditions. The spectra correspond to monomeric C_{70}, showing characteristic absorption peaks at 380 nm and 471 nm. This absorption is primarily attributed to $\pi \rightarrow \pi^*$ transitions. In these transitions, electrons are excited from bonding π-orbitals to anti-bonding π* orbitals within the conjugated carbon framework of C_{70}. Such transitions are characteristic of conjugated systems like fullerenes, where delocalized electrons facilitate absorption in the ultraviolet (UV) region. The specific nature of these transitions in C_{70} can be complex due to its molecular symmetry and electronic structure. Over time, the intensity of these absorption bands increases without any shift in their positions, highlighting that the aggregation process preserves the electronic structure and symmetry of the monomeric C_{70} molecules. This indicates that the increase in intensity results from aggregation, while the absence of a shift suggests that the formed aggregates retain the structural characteristics of the monomeric C_{70} molecule. The subsequent decrease in intensity observed on the 10^{th} day may be attributed to the fragmentation of C_{70} or structural changes that reduce its ability to absorb light. This is further supported by a decrease in the refractive index, indicating the formation of clusters. The increase in the absorption area reflects the growth in the number and size of clusters, which, in turn, leads to a decrease in the optical density of the solution over the given storage time.

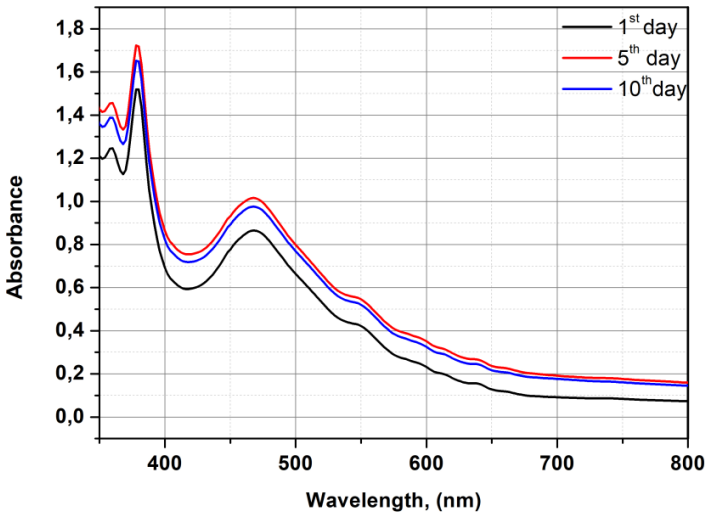

Fig. 1 – Changes in the UV-Vis absorption spectra of C_{70} in a xylene/tetrahydrofuran solution (volume ratio of xylene to tetrahydrofuran (0.95:0.05) as a function of storage time); initial C_{70} concentration: 0.2 mg/ml.

In summary, the spectral data confirm the enhanced aggregation of C_{70} in the xylene/tetrahydrofuran solution over time, affecting the absorption spectra. These

findings are crucial for understanding fullerene behavior in solution and the mechanisms of their aggregation.

3.2. THE DLS SPECTRUM

Figure 2 presents a DLS image of a in a xylene/tetrahydrofuran solution obtained at storage times. The graph shows that on day 1 (black line), the grain sizes are small, but the line width is much larger. This indicates that fullerene molecules at this storage time form a large number of clusters, with main sizes of 50, 100 and 145 nm. As the storage time increases to 5 days (red line), smaller particles aggregate to form larger nanoparticles with sizes of 100, 150, 215 and 360 nm. At 10 days of storage (blue line), fullerene molecules redistribute among the particles from the previous concentration, resulting in the formation of clusters with nearly uniform sizes of approximately 180 and 340 nm. The obtained results confirm that as the storage time increases, the total number of clusters decreases, but their average size grows. This process may be the result of interparticle interactions leading to the aggregation of smaller particles. It is also noteworthy that the changes in line width as a function of storage time highlight the heterogeneity in the size distribution of clusters in the solution. At the initial time (1^{st} day), a wide size range is observed, indicating the random nature of fullerene molecule aggregation. By the 5^{th} days, the aggregation becomes more organized, forming clusters with two primary sizes. Finally, after 10 days, the particles reach a stable state characterized by minimal size change. Thus, the analysis demonstrates the critical role of storage time in fullerene aggregation processes, which could be valuable for controlling cluster size and structure in various applications.

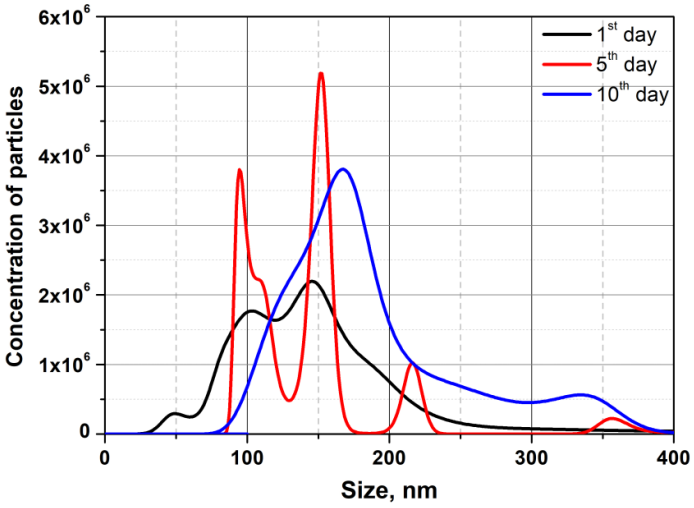

Fig. 2 – The DLS spectrum of the C_{70} xylene/tetrahydrofuran sample at different storage times. The fixed concentration of C_{70} fullerene in solution was 0.2 mg/ml.

3.3. THE RAMAN SPECTRUM

Raman spectroscopy proved to be an effective method for analyzing disorder in carbon-based materials. By examining specific features within the Raman spectra, it became possible to estimate the crystallite sizes in these disordered carbon structures. This Raman spectrum illustrates the evolution of the sample's structural and chemical properties over different storage times (1 day, 5 days, and 10 days). The Raman spectrum of the sample was analyzed, as presented in Figure 3. The Raman spectra exhibit prominent peaks, such as 178.6, 255.78, 503.75, 580.22, 733.14, 983.97, 1052.4, 1089.02, 1156.2, 1221.94, 1290.54, 1384.16, 1448.47, 2577.57, 2733.35, 2879.78, 2919.97 and 3047.07 sm^{-1} indicating vibrational modes specific to fullerene molecules, as well as 1581.39 and 1607.211 sm^{-1} vibrational modes specific to xylene molecules. These peaks are consistent across all time intervals. The peaks of the fresh solution (1 day) are relatively less intense, suggesting fewer structural interactions and possibly smaller or less aggregated clusters.

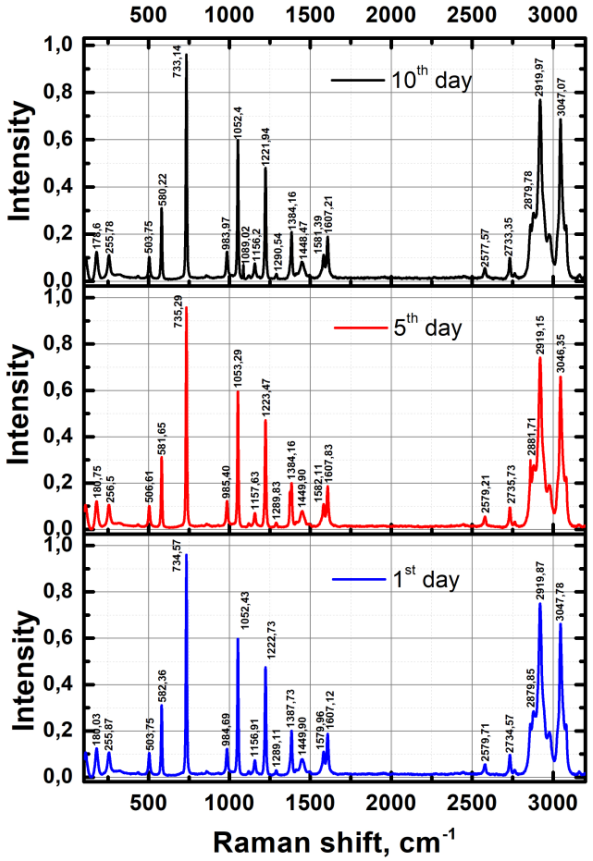

Fig. 3 – The Raman spectrum of the C_{70}/xylene/tetrahydrofuran sample at different storage times. The fixed concentration of C_{70} fullerene in solution was ~0.2 mg/ml.

The 5th day the intensity of several peaks increases, indicating enhanced interactions or the formation of larger aggregates. 10 days (blue line): decreased intensity, which may indicate that the aggregates have reached their maximum value during the aggregation process and have reached a more balanced state. Minimal or no significant shifts in peak positions are observed, implying that the fundamental molecular structure remains unchanged during storage. The changes in intensities, especially in higher vibrational modes (around 3000 cm^{-1}), suggest stronger intermolecular interactions or clustering over time. Raman analysis confirms that storage time significantly affects the aggregation properties of fullerene molecules. Over time, smaller clusters combine into larger, more stable structures, as evidenced by an increase in peak intensity at days 5 and 10 of storage. However, the lack of noticeable peak shifts indicates that these structural changes are primarily physical rather than chemical. This insight is valuable for applications requiring controlled aggregation states, such as sensor development, nanomaterial fabrication, and biomedical uses. Further studies could focus on quantifying these changes to optimize storage conditions for specific applications.

4. CONCLUSION

Obtained results show that C_{70} fullerene aggregates in xylene/tetrahydrofuran solutions even at low concentrations (0.2 mg/ml) at room temperature. Refractometry data indicate that fullerene molecules interact with solvent components, which leads to a change in their molecular structure and the formation of new compounds. With increasing storage time, the refractive index first increases and then decreases. This phenomenon is explained by the strengthening of intermolecular interactions and the onset of self-assembly of individual fullerene molecules. The observed decrease in solution density over time indicates a tendency of fullerene molecules to aggregate or form clusters.

Analysis of the UV-VIS absorption spectra of C_{70} in a binary solvent solution under different storage conditions shows a strong dependence of the spectral properties on the storage conditions. The characteristic peaks at 380 and 471 nm, corresponding to the C_{70} monomer, show red shifts and changes in absorption intensity after storage of the solution. The latter confirms the role of fullerene aggregation in these processes. DLS data confirm a decrease in the number of C_{70} particles and an increase in their average size over time. Raman spectra show that these structural changes are physical rather than chemical, with strong intermolecular interactions emerging as aggregation proceeds. These results emphasize the significance of interparticle interactions in driving the aggregation process and highlight the potential of using storage time as a parameter to control the size and structure of fullerene-based nanoclusters. This understanding is valuable for applications in nanomaterials, biomedical research, and drug delivery systems.

Aknowledgements. This work was supported by the Foundation for Fundamental Research of the Academy of Sciences of the Republic of Uzbekistan.

REFERENCES

1. L. Matija, R. Tsenkova, J. Munćan, M. Miyazaki, K. Banba, M. Tomić, and B. Jeftić, Adv. Mater. Res., **633**, 224–238 (2013).
2. M. Gokhale, R. Somani, Mini Rev. Org. Chem. **12**, 355–421 (2015).
3. A. Klinkova, H. Therien-Aubin, Nanochem. Res. **4**, 111–141 (2024).
4. M. Paukov, Ch. Kramberger, I. Begichev, M. Kharlamova, and M. Burdanova, Mater. **16**, 1276–1297 (2023).
5. T. Xu, W. Shen, W. Huang, and X. Lu, Mater. Today Nano **11**, 10008 (2020).
6. I.A. Avilova, V.A. Chernyak, Y.V. Soldatova, A.V. Mumyatov, O.A. Kraevaya, E.A. Khakina, P.A. Troshin, and V.I. Volkov, Int. J. Mol. Sci. **23**, 13344 (2022).
7. U.K Makhmanov, S.A. Esanov, B.A. Aslonov, and T.A. Chuliev, Adv. Nat. Sci: Nanosci. Nanotech. **16**, 025010 (2025).
8. J. Jin, X. Song, Z. Wang, X. Liu, L. Wang, J. Appl. Phys. **121**, 054305 (2017).
9. J. Paulo, V. Damasceno, D.W. Junior, F.B. Marques, L.T. Kubota, Electrochim. Acta. **483**, 144036 (2024).
10. U.K. Makhmanov, A.M. Kokhkharov, S.A. Bakhramov, S.A. Esanov, Rom. J. Phys. **67**, 601 (2022).
11. N.O. Mchedlov-Petrossyan, M.O. Marfunin, and N.N. Kriklya, Liq. **4**, 32–72 (2024).
12. S.-Q. Zhang, Z.-Y. Liu, W.-F. Fu, F. Liu, Ch.-M. Wang, Ch.-Q. Sheng, Y.-F. Wang, K. Deng, Q.-D. Zeng, L.-J. Shu, J.-H. Wan, H.-Z. Chen, and T.P. Russel, ACS Nano **11**, 11701−11713 (2017).
13. G. Niu, J. Geng, X. Wang, X. Yang, W. Xiong, H. Zhang, Z. Ruan, Y. Zhang, L. Gao, J. Lu, Nanotech. **34**, 395602 (2023).
14. U.K. Makhmanov, A.M. Kokhkharov, B.A. Aslonov, S.A. Esanov, Z. Bekmurodov, K.N. Musurmonov, A.X. Shukurov, T.A. Chuliyev, and A.N. Olimov, Nanomed. Nanotechnol. **9**, 000299 (2024).
15. Sh. Deguchi, R.G. Alargova, and K. Tsujii, Langmuir **17**, 6013–6017 (2001).
16. H.C. Chen, W.H. Ding, J. Chromatography A **1223**, 15–23 (2012).